Evaluation of Non-Linear Interference in Uncompensated Links using Raman Amplification

Evaluation of Non-Linear Interference in Uncompensated Links using Raman Amplification

V. Curri[(1)], A. Carena[(1)], P. Poggiolini[(1)], G. Bosco[(1)], F. Forghieri[(2)]

[(1)] *DET, Politecnico di Torino, Corso Duca degli Abruzzi, 24, 10129, Torino, Italy. curri@polito.it*
[(2)] *Cisco Photonics Italy srl, Via Philips 12, 20900, Monza, Italy. fforghie@cisco.com*

Abstract *We extend a model for nonlinear propagation over lumped-amplified uncompensated links to setups using Raman amplification. We compare theoretical to simulative results for PM-16QAM Nyquist-WDM on PSCF links, showing an excellent agreement. We also show that Raman NLI enhancement gives limited practical impairments in realistic setups.*

Introduction

Modern optical communications are fast evolving towards the use of multilevel modulation formats using coherent receivers based on digital signal processing (DSP)[1]. For such system scenarios it has been demonstrated that optimal setups are highly-dispersive uncompensated links[2]. To further increase spectral efficiency, a promising option is the use of Nyquist-WDM with channel spacing approaching the symbol-rate[3]. For this system category, it has been shown that fiber nonlinearities act introducing an additional Gaussian noise-like component called nonlinear interference (NLI)[4]. Theory allowing to analytically derive the amount of NLI in lumped-amplified links has been described and validated by simulations[4] and experiments[5].

With the increasing of cardinality of modulation formats, for instance moving from PM-QPSK to PM-16QAM, the use of hybrid Raman/EDFA amplification (HFA) seems to be the solution for achieving ultra long-haul distances[6].

In this work, we present the extension of NLI theory to setups based on Raman amplification. After introducing the theory, we validate it by comparing theoretical derivations to simulations of a Nyquist WDM PM-16QAM link made of pure silica-core fiber (PSCF). Simulation results display excellent agreement with theory.

Theory

We consider the transmission over a multi-span uncompensated link of N_{ch} Nyquist WDM channels at symbol rate R_s with channel spacing $\Delta f=R_s$ It can be shown that the power spectral density G_{NLI} of NLI on the center channel (worst-case) at the receiver can be expressed as[4]:

$$G_{NLI}=\frac{256}{27}\gamma^2 P_{Tx}^3 L_{eff}\int_0^{\frac{B_{opt}}{2}}\rho(\nu)|\nu|\frac{\sin^2\left(2N_s\pi^2\nu^2\beta_2 L_s\right)}{\sin^2\left(2\pi^2\nu^2\beta_2 L_s\right)}\log\left(\frac{B_{opt}}{2\nu}\right)\mathrm{d}\nu \quad (1)$$

where γ is the fiber nonlinear coefficient, P_{Tx} is the transmitted power per channel, L_{eff} is the fiber effective length, β_2 is the dispersion coefficient, L_s is the span length, N_s is the

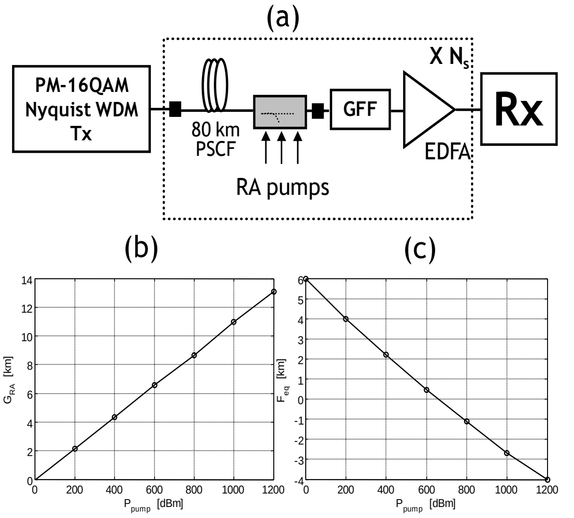

Fig. 1: Layout of the analyzed system setup (a), Raman on-off gain (b) and HFA equivalent noise figure (c) vs. overall pump power.

number of spans, $B_{opt}=N_{ch}\cdot R_s$ and ρ is the FWM efficiency[7]. Eq. (1) is obtained from the general expression of G_{NLI} reported in[4] (evaluated at $f=0$), with a proper change of variables based on the use of hyperbolic coordinates (e.g. $\nu^2=f_1\cdot f_2$). that holds for $\Delta f=R_s$.

In general, the FWM efficiency vs. phase-mismatch is given by[7]

$$\rho(\nu)=\frac{1}{L_{eff}^2}\left|\int_0^{L_s}p_{ch}(z)\exp\left\{j4\pi^2\beta_2\nu^2 z\right\}\mathrm{d}z\right|^2 \quad (2)$$

where $p_{ch}(z)$ is the normalized power evolution that depends on fiber loss coefficient α_s and on Raman pump evolution. Supposing counter-propagating and undepleted pump, $P_p(z)=P_{pump}\cdot\exp\{-\alpha_p(L_s-z)\}$, where α_p is the pump loss coefficient and P_{pump} is the launched pump power, $\rho(\nu)$ assumes the following close-form:

$$\rho(\nu)=\left(-0.23\frac{G_{RA}}{A_{fp}}\right)^{\left[-j\mathrm{N}^2\right]}\frac{\left|\left[\Gamma\left(-k_\alpha+j\mathrm{N}^2,-0.23\frac{G_{RA}}{A_{fp}}\right)-\Gamma\left(-k_\alpha+j\mathrm{N}^2,-0.23G_{RA}\right)\right]\right|^2}{\left\{\Gamma\left(-k_\alpha,-0.23\frac{G_{RA}}{A_{fp}}\right)-\Gamma\left(-k_\alpha,-0.23G_{RA}\right)\right\}^2} \quad (3)$$

where $\Gamma(s,x)$ is the upper-incomplete gamma-function[8], G_{RA} is the Raman on-off gain expressed in dB, $A_{fp}=\exp\{\alpha_p.L_s\}$, $k_\alpha=\alpha_s/\alpha_p$, $N^2=(2\pi)^2\beta_2\nu^2/\alpha_p$. Eq. (3) depends only on the overall Raman gain, therefore it is valid also for

multi-pump counter-propagating Raman setups provided that pump depletion is negligible. In case of relevant pump depletion, the analysis holds using Eq. (2) for $\rho(\nu)$ evaluation.
The system BER can then be derived from the non-linear OSNR[4], defined as:

$$OSNR_{NL} = \frac{P_{Tx}}{(G_{ASE} + G_{NLI})B_n} \qquad (4)$$

where G_{ASE} is the overall ASE noise power spectral density and B_n is the OSNR reference bandwidth.

Validation setup

In order to test the theoretical derivations, we analyze the system setup shown in Fig.1a. It is a N_s spans link carrying 11 PM-16QAM Nyquist-WDM channels at R_s=32 Gbaud and channel spacing $\Delta f=R_s$. Channels are electrically shaped using a Nyquist raised-cosine filter with *roll-off*=0.02 and an ideal DAC. The required OSNR in 0.1 nm in order to obtain the target BER=10^{-3} is 23 dB.
The system is composed of several spans of PSCF with length L_s=80 km. Each fiber span is followed by a coupler enabling counter-propagating Raman pumping, a gain flattening filter (GFF) that ideally compensates for the Raman gain tilting and an EDFA with noise-figure F=6 dB that recovers the residual loss. The PSCF parameters are: $\alpha_{s,dB}$=0.185 dB/km, $\alpha_{p,dB}$=0.3 dB/km, D=20.6 ps/nm/km (β_2=-26.2 ps^2/km) and γ=0.81 1/W/km. We include 5.2 dB of extra losses due to passive components and connectors in the span, hence we assume an overall span loss A_{span}=20 dB that is completely recovered by the HFA.
Raman amplification is obtained using three unpolarized counter propagating pumps at 1425, 1436 and 1459 nm. The overall pump power P_{pump} ranges from 200 mW up to 1200 mW. We limit P_{pump} to 1200 mW in order to have negligible depletion. As a reference, we also consider EDFA only lumped amplification (P_{pump}=0 mW).
Fig. 1b displays the Raman on-off gain G_{RA} vs. the overall pump power. The maximum value of G_{RA} is 13.1 dB for P_{pump}=1200 mW and it almost completely recovers the fiber loss that is 14.8 dB. Fig. 1c shows the values of the equivalent noise figure F_{eq} of the HFA for the different P_{pump} levels. While increasing P_{pump}, F_{eq} decreases from 6 dB for the case of EDFA only amplification to -4 dB for P_{pump}=1200 mW: it corresponds to an OSNR improvement of 10 dB.
We first apply the theory in order to evaluate the NLI enhancement $\sigma=G_{NLI}/G_{NLI,EDFA}$ of the NLI in cases of HFA with respect to EDFA-only amplification. Results are plotted in Fig. 2 as σ vs. P_{pump} for N_s=5 and N_s=30: the maximum value of σ is 2 dB, for P_{pump}=1200 mW. From these results it can also be deduced that the presence of Raman amplification, besides enhancing the NLI, slightly increases its accumulation along the line and does not increase linearly with P_{pump}. Such an effect is shown by the larger value of σ after 30 spans with respect to the one after 5 spans. We verified however that in all practical scenarios such an effect is limited to a small fraction of dB, as for the presented results, with a negligible impact on system performance.

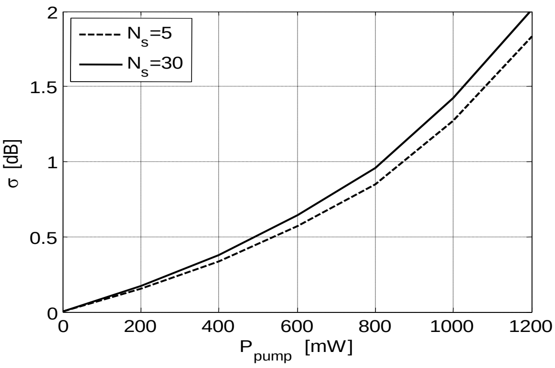

Fig. 2: NLI enhancement in Raman amplified links with respect to EDFA link for different overall Raman pumping after 5 and 30 spans

Simulative results

In order to validate the presented theory, we simulate the propagation of 11 PM-16QAM Nyquist-WDM channels in the link setup described in the previous section.
We use a polarization diversity Rx based on 90° hybrids and balanced photodetectors. The Rx electric bandwidth is ½·R_s=16 GHz and the local oscillator is supposed to be ideal, without phase noise. The Rx DSP placed after photodetectors operates at 2 samples/symbol and implements ideal electronic dispersion compensators and a butterfly equalizer based on 51-tap FIR filters. The filter coefficients are adjusted through a least mean squares (LMS) algorithm. Simulation results are obtained by simulating 2^{16} symbols (2^{19} bits) per channel and performing direct error counting on the center channel.
We vary the transmitted power per channel P_{Tx} from -5 up to +3 dBm. For each P_{pump} and P_{Tx} we derive the maximum reachable distance L_{max} still allowing BER≤10^{-3}. In order to isolate the effect of NLI enhancement due to Raman amplification, we also consider the *unrealistic* systems based on *equivalent*-EDFAs with noise-figures equal to the ones of the HFAs.
For each setup we also apply the proposed theory to derive the power P_{NLI} of NLI and consequently evaluate L_{max} at which $OSNR_{NL}$=23 dB (corresponding to BER=10^{-3}).

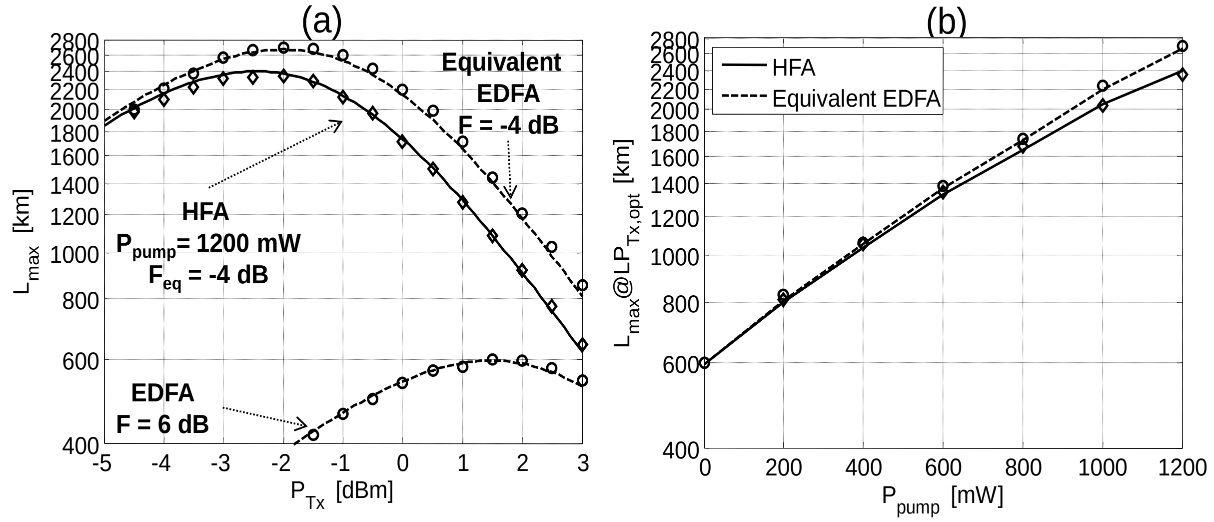

Fig. 3: Maximum reach L_{max} @ BER≤10^{-3} vs. the transmitted power (P_{Tx}) for EDFA only, HFA with P_{pump}= 1200 mW and its equivalent EDFA with F = -4 dB (a). Maximum reach @ BER≤10^{-3} for the optimal transmitted power vs. the overall Raman pump for HFAs and equivalent EDFAs (b). In both figures lines refer to theory, circles and diamonds to equivalent EDFA and HFA simulative results, respectively.

Fig. 3a shows results in terms of L_{max} vs. P_{Tx} for the EDFA-only link, for the 1200 mW HFA link and for its equivalent EDFA-only link. Lines refer to analytical results, while circles and diamonds are simulative results for EDFA-only and HFA links, respectively. The excellent agreement with simulative results confirms the accuracy of the proposed theoretical evaluation. On such a basis, together with other tests we have carried out and that are not reported here due to lack of space, we can conclude that the developed theory can reliably be applied to uncompensated links using Raman amplification and transmitting coherent modulation formats.

From Fig. 3a it can be also observed that using EDFAs with F=6 dB, L_{max}=600 km only, while, with 1200 mW HFAs, L_{max}=2400 km, corresponding to *4-times* (6 dB) on L_{max}. It is due to 10 dB ASE noise reduction (F_{eq} from 6 dB to -4 dB) and NLI noise enhancement inducing the optimal power $P_{Tx,opt}$ going from 1.5 dBm down to -2.5 dBm, i.e., 4 dB reduction. Moreover, we have seen in Fig. 2 that the 1200 mW HFA induces 2 dB NLI enhancement, corresponding (compare in Fig 3a, Eq. EDFA to HFA) to 0.5 dB reduction on both $P_{Tx,opt}$ and L_{max}. Hence, even with σ=2 dB, effects of NLI enhancement due to Raman amplification are limited.

Fig. 3b shows results as L_{max} at $P_{Tx,opt}$ for all the considered HFA setups and for their *equivalent*-EDFA links. As well as in previous plots, lines refer to theory while circles and diamonds are obtained by simulation. The excellent agreement between theory and simulations for all pump levels gives a further confirmation to the validity of the theory. Moreover, it can be observed that up to P_{pump}=800 mW, corresponding to σ=1 dB, effects of NLI enhancement are practically negligible. It indicates that, keeping the NLI enhancement below 1 dB, Raman amplification induces negligible impairments with respect to its equivalent-EDFA, i.e., we have benefits of noise reduction without excess NLI impact.

Note that, in general, for a fixed P_{pump}, σ decreases with the increasing of L_s. The reason is a reduction of the power at the end of the fiber span, where the Raman gain has higher effects. As a practical consequence, in most long-span links σ is smaller than 1 dB, giving a negligible impact on system performance.

Conclusions

We presented the extension of the theory of NLI for uncompensated links to systems based on Raman amplification. We showed general results and a specific close form for undepleted and counter-propagating pumps. Theory was successfully validated by simulation of Nyquist WDM PM-16QAM links on PSCF.

Acknowledgements

This work was supported by CISCO Systems within a SRA contract. The simulator OptSim® was supplied by RSoft Design Group Inc.

References

[1] M. G. Taylor, PTL, Vol. 16, p. 674, 2004
[2] M. S. Alfiad *et al*., JLT, Vol. 27, p. 3590, 2009
[3] G. Bosco *et al*., PTL, Vol. 22, p. 1129, 2010
[4] A. Carena *et al*., JLT, Vol. 30, p.1524, 2012
[5] E. Torrengo *et al*., Op.Exp., Vol. 19, p. B790, 2011
[6] Yamanaka *et al*., ECOC 2010, paper We.8.C.1
[7] N. Shibata, JQE, Vol. 23, p. 1205, 1987
[8] M. Abramowitz, I. A. Stegun, *Handbook of mathematical functions*, 1965